Neutron imaging versus standard X-ray densitometry as method to measure tree-ring wood density

Author(s):
Mannes, David; Lehmann, Eberhard; Cherubini, Paolo; Niemz, Peter

Publication date:
2007

Permanent link:
https://doi.org/10.3929/ethz-b-000005205

Originally published in:
Trees 21(6), https://doi.org/10.1007/s00468-007-0149-8

Trees (2007) 21:605–612
DOI 10.1007/s00468-007-0149-8

ORIGINAL PAPER

Neutron imaging versus standard X-ray densitometry as method to measure tree-ring wood density

David Mannes · Eberhard Lehmann · Paolo Cherubini · Peter Niemz

Received: 17 July 2006 / Revised: 14 May 2007 / Accepted: 15 May 2007 / Published online: 14 June 2007

Abstract Neutron imaging is a new non-destructive testing method in wood science. It is similar to X-ray methods but with differing sensitivities for different elements. In this study, neutron imaging was used to ascertain the density profiles of thin spruce samples and compared with results generated with standard X-ray microdensitometry. Data obtained through neutron imaging were similar to those resulting from the X-ray method. The advantage of neutron imaging is its higher sensitivity to some elements such as hydrogen. Together with the high neutron-sensitivity of the applied detectors (imaging plates) this makes shorter exposure times possible, and yields more detailed information on the inner composition of wood. X-ray film, which is still most commonly used in X-ray densitometry, has the disadvantage that the relationship between the optical density of the film and the density of wood is non-linear. This means that corrections and calibration with step wedges are necessary, whereas with neutron imaging the digital values can be used directly to calculate the density at a certain point of the specimen. Thus neutron imaging appears to be an appropriate method, which can be used as complement to established X-ray methods for fast and straightforward investigations of tree rings, growth zones and wood density.

Keywords Neutron imaging · X-ray densitometry · Wood density · Tree-ring analysis · Dendrochronology

D. Mannes (✉) · P. Niemz
Institute for Building Materials, ETH Zurich,
CH-8093 Zurich, Switzerland
e-mail: dmannes@ethz.ch

D. Mannes · E. Lehmann
Paul Scherrer Institute, CH-5232 Villigen, Switzerland

P. Cherubini
WSL Swiss Federal Institute for Forest,
Snow and Landscape Research,
CH-8903 Birmensdorf, Switzerland

Introduction

Wood density is one of the most important wood characteristics for assessing wood quality as it provides an indication of the physical and mechanical properties of wood, such as strength, stiffness, hardness, hygroscopic properties, swelling and shrinkage processes, thermal conductivity and acoustic properties (Kollmann and Côté 1968). Moreover, variations in the wood density inside and between tree rings can provide valuable information on past climatic conditions and on tree carbon storage at a site under natural or artificial conditions (Hughes 2002). For example, it might show the influence of fertilisation or air pollution on carbon sequestration by trees (Bascietto et al. 2004).

Tree-ring analysis, i.e. the measurement of ring width and wood density, is the first essential step in a dendrochronological study. It relies on the characteristic succession of earlywood and latewood, as well as their density, within and across the tree rings to date the formation of wood rings. The analysis of these rings makes it possible to reconstruct past environmental conditions. In particular, variations in tree-ring density have been widely used for dendroclimatological purposes because maximum density has been found to be one of the best climatic proxies with annual resolution for reconstructing past summer air temperatures, which are relevant for the discussion of current climatic change (IPCC 2001).

There are many methods for determining wood density, but there is now increasing interest in developing new methods, yielding more detailed information in shorter time. One option is to perform optical analyses using digital cameras to record light reflected or transmitted by the specimens and subsequently perform a computer-based analysis of the resulting image (Clauson and Wilson 1991). This might be applied down to a microscopic level (Park and Telewski 1993), but does not necessarily work out for all wood species, particularly for those characterised by conspicuous differences between sapwood and coloured heartwood (Sheppard et al. 1996). Another optical approach is to measure the cell wall thickness on a microscopic level (transmission light microscope) and then to assess the wood density of the tree ring (Decoux et al. 2004). As Koch et al. (1998) showed light in the far infrared spectrum can be used to evaluate wood density.

A non-optical method is to measure the drilling resistance to ascertain density variations within and between tree rings (Rinn et al. 1996). A rather destructive way of measuring wood density is the laser-sandblasting method, which relies on the correlation between hardness and wood density (Schulz 1985). Larger amounts of the less dense earlywood are abraded, leaving a characteristic profile on the sample which can be scanned and registered with a laser (Lesnino 1994). A new non-destructive testing method is high-frequency densitometry, which uses variations in the dielectric properties of wood to detect wood density alterations (Schinker et al. 2003).

The most common and widely accepted methods are, however, based on radiographic measurements. The first tests with ionising radiation were made in the late 1950s with β-rays (Cameron et al. 1959) and γ-rays, which are still used (Tiitta et al. 1996). X-rays are, however, the most common method based on radiographic measurements. X-ray radiography of wood was developed in the 1960s, mainly by Polge (1964, 1965, 1966), and adopted by several other wood-technology laboratories (Lenz et al. 1976; Polge 1978). The method, which has not changed significantly since the sixties, is described by Schweingruber et al. (1978) and Eschbach et al. (1995). The X-ray densitometry is based, in most instances, on X-ray films, which are analysed with a densitometer. Earlier attempts were made to use computerised data processing in the analyses (Parker et al. 1973) and to directly scan in data (Hoag and McKimmy 1988; Moschler and Winistorfer 1990; Bergsten et al. 2001). The majority of investigations today are nevertheless still based on the evaluation of X-ray films (Koenig et al. 2005). One problem which occurs while using X-ray film is the nonlinearity of the relationship between the optical density and the actual wood density (Rudman et al. 1969; Lenz et al. 1976). Corrections and calibrations have therefore to be made based on step wedges with similar density, and thus a presumably similar beam attenuation as wood.

Neutron imaging (NI) is a new non-destructive method which works according to the same principles as X-ray. It provides information on the inner structures and the constitution of samples, and is strongly correlated with the density and the moisture content of the material being examined. As neutrons are more sensitive than X-ray to some elements like hydrogen, it is particularly suitable for investigating wood (Lehmann et al. 2001). Moreover, neutron imaging is nowadays based on digital data acquisition, so that there is a linear correlation between the image data and the effective density of the material being tested, as well as a shorter acquisition time.

We present here a comparative study of methods for analysing tree rings, with the main focus on comparing standard X-ray methods and neutron imaging.

Materials and methods

Neutron imaging—General principles

Both neutron imaging (NI) and X-ray radiography are based on the principle of transmission measurement. From a source (in this case the spallation neutron source SINQ at the Paul Scherrer Institut (PSI), Villigen, Switzerland) low energy neutrons are guided via a collimator on a specimen. Depending on the constitution and inner structure of the specimen, the neutron beam is attenuated and subsequently registered behind the sample as a two-dimensional data set of grey-level values in individual pixels by a detector system. Unlike X-rays where the photons interact with the electron shells of the atoms, the neutron beam interacts with the nuclei of the atoms within a sample. Hence different elements have different interaction probabilities with the neutrons, providing information on the constitution of the specimen.

Despite the differences between X-ray and neutron imaging, the basic principles are the same. The following explanations of neutron functionality can be applied similarly to X-rays. The main formal difference is in the nomenclature, namely of the attenuation coefficients, which is Σ for neutrons and μ for X-rays.

For the following considerations, energy dependence of the radiation was completely ignored. In accordance with the attenuation law, the intensity of the neutron beam behind the sample can be calculated as follows:

$$I = I_0 \cdot e^{-\Sigma \cdot d} \quad (1)$$

where, I_0 is the incident intensity of the neutron beam (grey levels); I is the weakened intensity of the neutron beam

(grey levels); Σ is the attenuation coefficient (cm^{-1}); d is the sample thickness (cm).

Based on this equation, the attenuation coefficient Σ can be calculated by:

$$\Sigma = \frac{\ln\left(\frac{I_0}{I}\right)}{d} \quad (cm^{-1}) \tag{2}$$

The attenuation coefficient is determined by the nuclear density N and the interaction probability σ for the respective elements constituting the sample. The effective attenuation coefficient Σ_{eff} consists of the attenuation coefficients of the involved elements and can thus also be described as follows:

$$\Sigma_{eff} = \sum_{i=i}^{n} N_i \sigma_i \quad (cm^{-1}) \tag{3}$$

where, N is the nuclear density (nuclei/cm^3); σ is microscopic cross-section interaction probability with the neutrons (cm^2)

If:

$$N_i = \frac{\rho_i}{M_i} \cdot L \quad (nuclei/cm^3) \tag{4}$$

where, ρ is the density (g/cm^3); L is the Avogadro's constant; M is the atomic weight (g/mol); the density ρ can be calculated by

$$\rho = \frac{\Sigma M}{L\sigma} \quad (g/cm^3) \tag{5}$$

If the elemental composition and the microscopic cross-sections, i.e. the interaction probabilities of the incident neutrons with the elements present in the material examined, are known, the density of a sample can be determined with the above Eq. (5). The chemical composition of different wood species varies considerably especially with regard to their respective lignin/cellulose ratio and the types of lignin, but their composition as far as chemical elements are concerned is practically identical (Lohmann et al. 2003). The wood of most tree species consists mainly of the elements C, H, O and N in similar proportions for most tree species (Table 1). Small traces of other elements can also be found, and these are species specific. They represent, however, only a very small part of the elements.

In our study, the main focus was on the four major elements, and the remaining elements were ignored. The microscopic cross-section σ of wood was calculated with the mean values of the spectrum of the NEUTRA facility at PSI (Lehmann et al. 1999) for the elements concerned. With these values a weighted microscopic cross-section for wood was calculated, based on the proportions of the elements C, O, H and N occurring in wood. The macroscopic cross-section and the attenuation coefficient Σ were calculated with the data of the neutron image. These values were used to calculate the wood density profile using Eq. 5.

The incident beam can be transmitted, scattered or absorbed by the atoms within the sample. Scattering and absorption of neutrons are both comprised in the attenuation coefficient or macroscopic cross-section (Σ). The simple exponential attenuation law applies only as a first approximation. Specimens that are thicker in the direction of the beam direction or made of a highly scattering or absorbing material lead to deviations from this approximation. Wood, which is basically composed of compounds of C, O, H and N, normally shows scattering as main interaction with the neutron beam. Because of the relatively small dimensions of the specimens tested, namely 1 mm in the direction of the beam, no secondary scattering was expected, and no calculative scattering correction deemed to be necessary. Small distances between the specimen and the detector, which were here only a few millimetres, still may have an influence on scattering, and so have to be considered.

Neutrons and X-rays have different interaction probabilities and thus different sensitivities to different elements. The attenuation coefficient for spruce wood is for neutrons about 10 times higher than for X-rays with 160 kV (Mannes 2006). The attenuation coefficients confine the

Table 1 Wood in a simplified physical model. The microscopic cross-sections of the neutrons are the average values of the energy spectrum at the NEUTRA facility at PSI

Elements	% by weight	Atomic weight M (g/mol)	Nuclear density N (nuclei/cm^3)	Microscopic cross-section for thermal neutrons at PSI σ (cm^2)	Attenuation coefficient for thermal neutrons Σ (cm^{-1})
C	50	12.01	1.10e + 22	4.92e – 24	0.56
O	43	16	7.21e + 21	4.00e – 24	0.17
H	6	1.01	1.57e + 22	4.58e – 23	3.44
N	1	14.01	1.89e + 20	1.18e – 23	0.43
Total	100			6.65e – 23	4.60

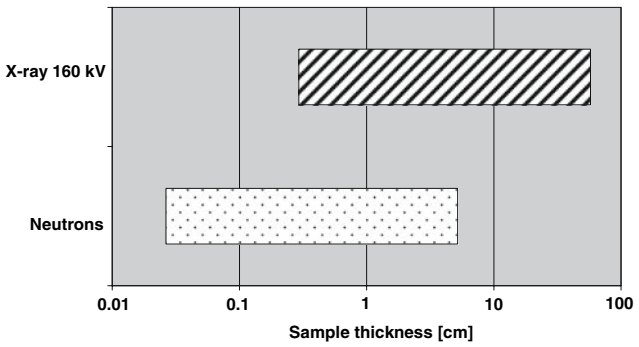

Fig. 1 Theoretical sample thickness of spruce wood in the beam direction (ρ = 0.44 g/cm^3) for X-rays (160 kV) (*above*) and thermal neutrons (*below*) on a logarithmic scale

maximum and minimum sample thickness of a material which can be reasonably examined with a detector-system. This is on its part defined by its dynamic range and the detection noise. As can be shown in Fig. 1, the sample dimensions that can be tested with neutrons are an order of magnitude below those of X-rays with 160 kV. This makes the method of neutron radiography particularly suitable for tree-ring analyses, where the sample thickness is normally relatively small in order to avoid oblique fibre orientation. This would otherwise lead to blurred images and thus to errors in the determination of the tree-ring border and the density distribution.

Neutron-sensitive imaging plates (IP) were applied as a detector system in this study. This detector system is based on the phenomenon of photo-stimulated luminescence (PSL), which is based on the interaction between ionising radiation like X-rays and a layer of photostimulable crystals. A detailed description of the method can be found in Amemiya and Miyahara (1988). The imaging plates used for neutron imaging purposes also contain Gadolinium (Gd), which acts as a neutron converter (Tazaki et al. 1999).

After exposure to the neutron beam, the latent information stored on the imaging plate was extracted and digitised by means of a special imaging-plate-reader (e.g., Fujifilm BAS-2500). The resolution of the reader was 50 µm per pixel. In the readers used here, the imaging plates are scanned with a laser and the emitted light is amplified with a photomultiplier and subsequently digitised. Results from this procedure are 16-bit images with up to 65'536 grey-level values. In the presented case, the employed detector and experimental setup showed a signal-to-noise-ratio (S/N) of approximately 100.

The facility used for the present investigations was the Neutron Radiography Station (NEUTRA) at the PSI, which relies on thermal neutrons (25 meV) (Lehmann et al. 1999).

Radiography of standard specimens

We used Norway spruce (*Picea abies* (L.) Karst.) samples in a first series of tree-ring analyses. The samples were obtained from trees that had been bent in the winter 1981/1982 by a snow avalanche in a forest plantation at Blesa/Pusserein, close to Schiers (Grisons, Switzerland). The response of the trees, during recovery was observed until 1994, and the trees were then cut down (19 July 2004) as part of a long-term study of the interrelationships between trees and avalanches (Frey 1984). From each of six trees, three stem disks were obtained, at three different heights (at 5, 50, 100 cm height). From each disk, we cut two opposite samples (2 cm wide) along the rays, including the pith. All the samples were analysed using X-ray microdensitometry. The samples were 1 mm thick. The X-ray densitometric investigations were carried out at the Swiss Federal Institute for Forest, Snow and Landscape Research (WSL), using the densitometer Dendro 2003 (Walesch-Electronics, Effretikon, Switzerland), described in Eschbach et al. (1995).

For the neutron radiographic investigations, the samples were first fixed on a sheet of paper and then attached directly to an imaging plate. This was then placed inside the radiography station in front of the flight tube, which conducts the neutrons from the source into the experimental chamber (Fig. 2). The imaging plates were positioned approximately 11 m away from the aperture and 13 m from the centre of the source ($L/D \approx 500$).

The imaging plates were exposed for 20 s. After extraction and digitisation of the images, the data obtained (Fig. 3) were analysed with special image processing software (Aida Image Analyzer v.3.11). This was done by laying a profile where a wood strip could be seen in the image. It was attempted to position the profile analogue to the measuring points used for the X-ray microdensitometry. The integrated profile, which had a width of 2 mm, was drawn perpendicular to the tree rings. The grey-level values were integrated over the width of the profile, yielding a value series representing the transmitted neutron beam behind the sample (I). The ''open beam'' or the incident beam (I_0) was ascertained with values from areas close to the profiles laid over the wood samples (Fig. 3). With the data for I and I_0, it was possible to determine the attenuation coefficient Σ of the sample (cf. Eq 1) and to subsequently calculate the wood density along the line profile.

The data from the neutron radiographic analysis were subsequently compared with data obtained from X-ray microdensitometry. Those measurements were carried out at WSL. The X-ray images were produced with 12 kV and 20 mA and an exposure time of 88 min. After developing the film, the X-ray images were evaluated with the microdensitometer Dendro 2003 (Eschbach et al. 1995).

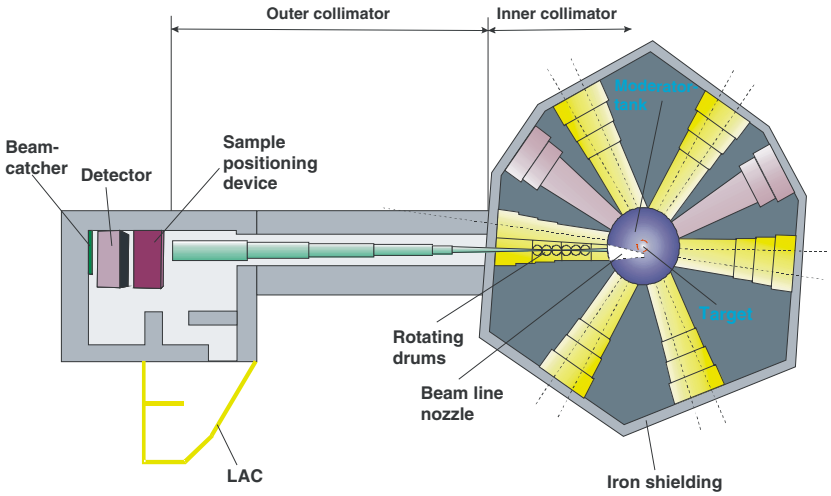

Fig. 2 Sketch of the neutron radiography station NEUTRA with thermal neutrons

This generated density values from the grey-level values of the image after a calibration with a step wedge. These density values were used for a comparative evaluation of the neutron data. For this purpose, the two data series obtained for a specific sample with means of the described methods were joined and their course fitted manually using the respective density maxima of the late wood areas as fixed points. This data set was subsequently used to calculate the correlation coefficient r for the wood density ascertained with neutron imaging and X-ray.

Results and discussion

The results obtained from imaging with thermal neutrons tend to correlate closely with the density allocations ascertained with X-ray densitometry (Fig. 4) showing a high correlation coefficient r of 0.96 (Fig. 5). This correlation study was conducted with the two respective density values determined for the individual measuring points within the sample. As the results were ascertained in two independent measuring campaigns by two different research groups, it was not possible to re-establish the exact location of all measuring points and thus the resulting density profiles had to be fitted manually in all conscience. Still the resulting density profiles determined by using the two methods are mostly consistent with each other.

Although the neutron curve is slightly beneath the X-ray curve, it appears less noisy and shows the structure more clearly. This is probably mainly due to the fact that the samples were fixed directly on the detector, so that neutrons scattered by the sample and the paper on which they were fixed led to the assumption of a slightly higher transmission than there really was.

The two curves differed slightly in some parts and some of the amplitudes of the neutron gradient appear higher than those from the X-ray data. It is possible that, in these areas of the sample, different components are crucial for the attenuation with the two radiation forms, as they have different interaction probabilities for the same elements, in particular for hydrogen. As can be seen in Fig. 4, the neutron curve is much smoother and appears less noisy than the X-ray curve. This may be partly due to the higher resolution for the X-ray data, as the sensor aperture had a width of just 10 µm whereas the pixel size in the neutron radiographs is 50 µm, which might be reduced to 12.5 µm by the use of an improved IP-reader.

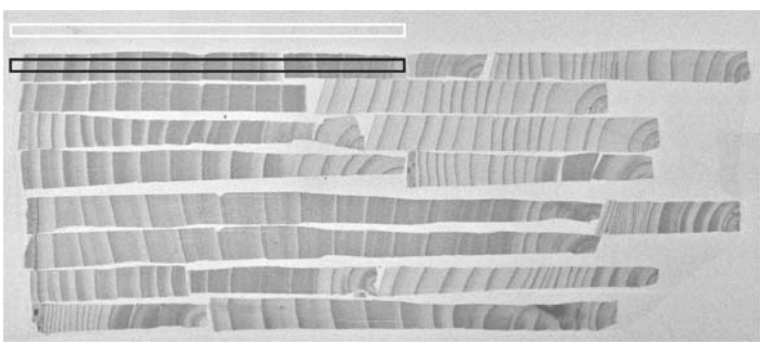

Fig. 3 Neutron radiographic image of spruce samples used for the analysis; on the basis of 2 mm wide profiles, the values for the transmitted beam I (*black*) and the incident beam I_0 (*white*) were ascertained

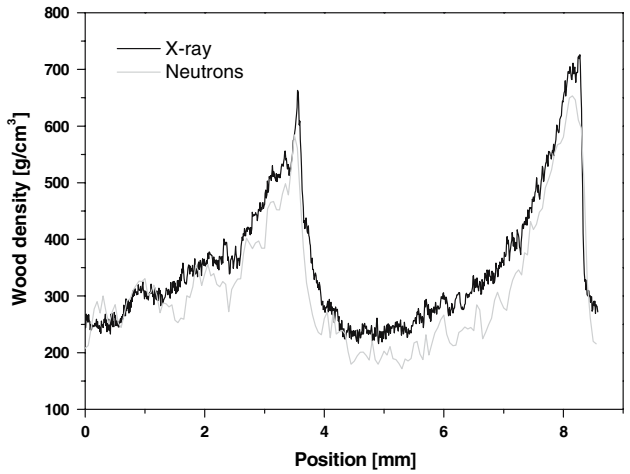

Fig. 4 Section of density profiles ascertained with standard X-ray microdensitometry (*black*) and by means of neutron imaging (*grey*). Both have similar characteristics, although the neutron curve is slightly lower than the X-ray curve

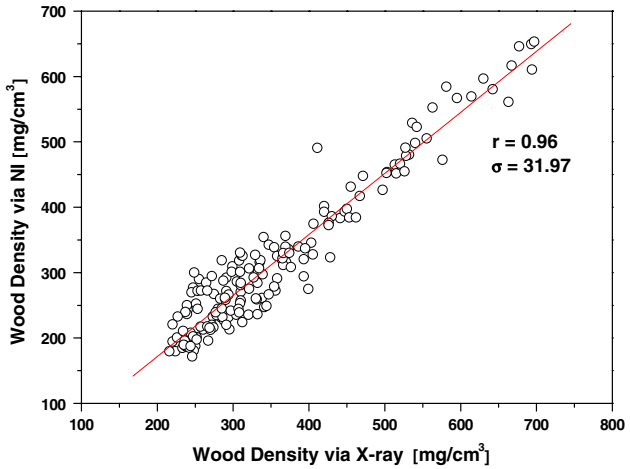

Fig. 5 The comparison of the wood density ascertained with X-ray microdensitometry (*X-axis*) and neutron imaging (NI) (*Y-axis*) for the individual measuring points of Fig. 4 shows a linear correlation (*straight line*); the correlation coefficient r accounts for 0.96, the standard deviation σ for 31.97

Another factor which might be responsible for some of the differences is that, while the probing slit was always adjusted parallel to the tree ring borders for the X-rays, it was fixed for the neutron images. As the tree rings were not always parallelly aligned, and as the tree rings had smaller radii towards the pith, some parts of the tree rings crossed the profile line obliquely. This leads to a certain fuzziness in the tree-ring borders, making it moreover difficult to align the peaks of the two curves. The latter was hampered by the fact that the exact position of the X-ray measurement could not be entirely reconstructed.

The noisy appearance of the curve based on the X-ray data may also have been caused by the fact that the geometry of the X-ray beam was not parallel but fan-shaped. This increases the difficulties and possible sources of error considerably. With the neutron facility, however, this was not a problem as it provides a virtually parallel neutron beam at the position of the samples, which in turn decreases the noise. The parallel beam is due to the relatively large distance between source and detector as well as the collimation.

Another factor which has to be taken into account in comparing the two methods is time. Preparing the samples is equally time consuming for both methods and cannot be done quicker without loss of quality. The greatest differences occur in the exposition time for imaging. This period takes approximately 20 s for neutron radiography, but 88 min for the X-ray. Additionally, it takes time to develop the X-ray film and to ascertain the density data from the film with the densitometer. In contrast acquisition for neutron imaging is complete when the imaging plates are read with the IP-scanner, after which the extraction of the data takes another 2 to 3 min. If a different detector system like a scintillator-CCD-camera system is used, the whole acquisition procedure is finished by the end of the exposition time (Schillinger et al. 2005). On the other hand, this system shows a lower resolution than the imaging plates. The result is in each case a digital image, which is then the base for further analysis.

Conclusions

Neutron imaging is a practical method for determining wood density, and a good alternative to standard X-ray methods. It has several advantages over conventional X-ray radiography, which, in most cases, is still based on X-ray films. Due to higher attenuation coefficients for the major elements, in particular hydrogen, constituting the wood structure, neutrons have a greater sensitivity for wood than X-rays amounting to a whole order of magnitude. This means that small samples can be examined more quickly. For comparable results with X-rays, low voltages with long exposure times would be necessary. A further disadvantage of the X-ray method is that it is still based on X-ray film, which means that additional time is needed to develop the film and digitise the data, which means less samples can be tested within a day. Moreover with X-ray film, the optical density and effective wood density are nonlinear which makes several corrections and calibrations with a step wedge necessary. The data from neutron imaging on the other hand can be directly used for further analyses including to determinate the wood density at a certain point in the sample. Although neutron imaging has advantages, there are still some problems. The sensitivity of the neutron beam is greater for the elements contained in

Table 2 Comparison of the main features of neutron imagining and X-ray microdensitometry

Neutron imaging	X-ray microdensitometry
• High sensitivity: – shorter exposition time – examination of smaller sample dimensions possible (but at the same time constraint at the upper limit)	• Low sensitivity for wood components: – long exposition times – examination of big samples possible (examination of small samples limited)
• Direct evaluation of the data due to exclusive utilisation of digital detector systems	• Standard X-ray microdensitometry based on X-ray film → additional calibration and digitisation necessary
• Few specialized facilities available (Neutron source with Radiography/Imaging station)	• While standard X-ray equipment is very common, the special X-ray microdensitometry equipment is not thus availability scarcely higher than for neutron imaging
• Costs at PSI: – approved research proposals usually cost-free – fixed tariffs for commercial or industrial requests	• Costs: Fixed tariffs according to the institutions conducting the tests

wood, which means that the size of the samples that can be examined in this way is limited. For larger samples scattering correction may also be necessary. Another potential problem is the limited availability of facilities where neutron-imaging experiments can be conducted. X-ray densitometry is, however, also not widespread, because the equipment is still expensive and there are only a few institutes with the necessary equipment.

The costs of the respective experiments are not easy to specify. Neutron imaging can only be conducted at few large-scale research facilities, where experiments can be applied via research proposals. These are usually cost-free, only commercial and industrial requests are charged fixed tariffs.

A compilation of the main features of the two methods can be seen in Table 2. Despite these problems, neutron imaging is still a very useful investigative method for examining properties of wood. Further testing would, therefore be appropriate. Thermal neutrons provided satisfactory results for studying the small specimens examined here, but low energetic neutrons would probably produce higher contrasts and would thus be more suitable for tree ring analyses. Resolution might be enhanced by the utilisation of improved detector-systems / -equipment like new IP-scanners with a readout pixel-size of 12.5 μm or a microtomography-facility working with cold neutrons. Noise might be reduced and thus reliability of the data increased by the implementation of scattering correction algorithms based on Monte-Carlo simulations.

References

Amemiya Y, Miyahara J (1988) Imaging plate illuminates many fields. Nature 336(6194):89–90

Bascietto M, Cherubini P, Scarascia-Mugnozza G (2004) Tree rings from a European beech forest chronosequence are useful for detecting growth trends and carbon sequestration. Can J For Res 34:481–492

Bergsten U, Lindeberg J, Rindby A, Evans R (2001) Batch measurements of wood density on intact or prepared drill cores using x-ray microdensitometry. Wood Sci Technol 35:435–452

Cameron JF, Berry PF, Phillips EW (1959) The determination of wood density using beta rays. Holzforschung 13:78–84

Clauson ML, Wilson JB (1991) Comparison of video and x-ray for scanning wood density. For Prod J 41(3):58–62

Decoux V, Varcin E, Leban JM (2004) Relationship between the intra-ring wood density assessed by X-ray densitometry and optical anatomical measurements in conifers. Consequences for the cell wall apparent density determination. Ann For Sci 61:251–262

Eschbach W, Nogler P, Schär E, Schweingruber FH (1995) Technical advances in the radiodensitometrical determination of wood density. Dendrochronologia 13:155–168

Frey W (1984) Durch schneelast verursachte schäden in den fichten-aufforstungen von bleisa/pusserein 1981/82. Analyse, folgerungen, behandlungsvorschläge. Interner bericht Nr. 619, Eidgenössische Institut für Schnee- und Lawinenforschung, Davos, Switzerland

Hoag M, McKimmy MD (1988) Direct scanning x-ray densitometry of thin wood sections. For Prod J 38(1):23–26

Hughes MK (2002) Dendrochronology in climatology—the state of the art. Dendrochronologia 20:95–116

IPCC (2001) Climate change 2001: synthesis report. In: Watson R.T. and the Core Writing Team (eds) Cambridge University Press, Cambridge, UK

Koch M, Hunsche S, Schumacher P, Nuss MC, Feldmann J, Fromm J (1998) THz-imaging: a new method for density mapping of wood. Wood Sci Technol 32:421–427

Koenig J, Guenther B, Bues CT (2005) New multivariate cross-correlation analysis. TRACE 53(3):159–166

Kollmann FFP, Côté WA Jr (1968) Principles of wood science and technology. Vol. I: solid wood. Springer, Heidelberg, p 592

Lehmann E, Vontobel P, Wiezel L (1999) Properties of the radiography facility NEUTRA at SINQ and its potential for use as European reference facility. Proc. 6th World Conf. On Neutron Radiography, Osaka 1999

Lehmann E, Vontobel P, Scherrer P, Niemz P (2001) Anwendung der methode der neutronenradiographie zur analyse von holzeigenschaften. Holz als Roh- Werkstoff 59:463–471

Lenz O, Schaer E, Schweingruber FH (1976) Methodische probleme bei der radiographisch-densitometrischen Bestimmung der Dichte und der Jahrringbreiten von Holz. Holzforschung 30:114–123

Lesnino G (1994) The laser-sandblasting method: a new method for the qualitative annual ring analysis of conifers. Wood Sci Technol 28:159–171

Lohmann U, et al. (2003) Holz-Lexikon, 4th edn., vol I. DRW, Leinfelden-Echterdingen

Mannes D (2006) Investigation of wood properties by means of neutron imaging techniques. Proc. 6th International PhD Symposium in Civil Engineering, Zurich 2006

Moschler WW, Winistorfer PM (1990) Direct scanning densitometry: an effect of sample heterogeneity and aperture area. Wood Fiber Sci 22(1):31–38

Park WK, Telewski FW (1993) Measuring maximum latewood density by image-analysis at the cellular level. Wood Fiber Sci 25(4):326–332

Parker ML, Schoorlemmer J, Carver LJ (1973) Computerized scanning densitometer for automatic recording of tree ring width and density data from X-ray negatives. Wood Fiber 5(3):237–248

Polge H (1964) Structural analysis of wood by densitometric studies of radiographs. Joyce Loebl Review

Polge H (1965) New investigations on wood by densitometric analysis of radiographs. Joyce Loebl Review

Polge H (1966) Etablissement des courbes de variation de la densité du bois par exploration densitométrique de radiographies d'échantillons prélevés à la tarière sur des arbres vivants. Applications dans les domains technologiques et physiologiques. PhD Thesis University of Nancy (F)

Polge H (1978) Fifteen years of wood radiation densitometry. Wood Sci Technol 12:187–196

Rinn F, Schweingruber FH, Schär E (1996) Resistograph and X-ray density charts of wood comparative evaluation of drill resistance profiles and X-ray density charts of different wood species. Holzforschung 50(4):303–311

Rudman P, McKinnell F, Higgs M (1969) Quantitative determination of wood density by X-ray densitometry. J Inst Wood Sci 24(6):37–43

Schillinger B, Abele H, Brunner J, Frei G, Gähler R, Gildemeister A, Hillenbach A, Lehmann E, Vontobel P (2005) Detection systems for short-time stroboscopic neutron imaging and measurements on a rotating engine. Nucl Instrum Methods Phys Res A 542(1–3):142–147

Schinker MG, Hansen N, Spiecker H (2003) High-frequency densitometry—a new method fort he rapid evaluation of wood density variations. IAWA J 24(3):231–239

Schulz H (1985) Härteprofile als Hinweis auf verschiedene Festigkeitssysteme im Holz. Holz als Roh Werkstoff 43:212–222

Schweingruber FH, Fritts HC, Bräker OU, Drew LG, Schär E (1978) The X-ray technique as applied to dendroclimatology. Tree-Ring Bull 38:61–91

Sheppard PR, Graumlich LJ, Conkey LE (1996) Reflected-light image analysis of conifer tree rings for reconstructing climate. Holocene 6(1):62–68

Tazaki S, Neriishi K, Takahashi K, Etoh M, Karasawa Y, Kumazawa S, Niimura N (1999) Development of a new type of imaging plate for neutron detection. Nucl Instrum Methods Phys Res A 424:20–25

Tiitta M, Olkkonen H, Kanko T (1996) Veneer sheet density measurement by the ^{55}Fe gamma attenuation method. Holz als Roh Werkstoff 54:81–84